AN ANALYSIS OF THE EFFECT OF HOLES PATTERNS ON COUPLED INSTABILITY OF PERFORATED THIN-WALLED MEMBERS

MIHAI NEDELCU*

Abstract. The buckling behaviour of vertical steel pallet rack columns is greatly influenced by the distribution of perforations punched continuously along their length. To study the influence of the holes patterns on the elastic coupled instabilities of thin-walled members, this paper uses an original modal identification method (based on the Generalised Beam Theory) which is able to provide the pure buckling modes participation (of global, distortional, local nature) in a general eigenvalue buckling mode given by the shell Finite Element Analysis.

Key words: rack columns, perforated thin-walled member, interactive buckling, mode decomposition, shell finite element analysis, generalised beam theory.

1. INTRODUCTION

The perforated thin-walled members are often used in civil and mechanical engineering as highly efficient load bearing components. A special case is represented by the cold-formed steel pallet rack columns, and the assessment of their resistance capacity is a particularly difficult problem in structural engineering. The perforations are punched continuously along their length to enable horizontal storage rack shelving to be clipped into position at arbitrary levels (Fig. 1) and these perforations decrease the rack column's axial capacity. Also, their typical slenderness leads to a failure mechanism usually governed by coupled instabilities (or interactive buckling). To study these complex phenomena one usually starts with the fundamental (pure) buckling types, widely accepted as: Global (rigid-body behaviour of the cross-section in its plane, yielding to flexural or flexural–torsional buckling), Distortional (relative transversal displacements between the cross-sectional corners) and Local (only local plate deformations) buckling (GDL). Each buckling type has its characteristic post-buckling behaviour and strength reserve; consequently, the derivation of the pure modes participation to a general buckling mode is a crucial step in assessing the real design resistance of the member.

Nowadays there are a number of specialized methods capable to provide the modal identification and participation, the most famous being the Generalised

* Technical University of Cluj-Napoca, Faculty of Civil Engineering, Romania

Beam Theory (GBT) [1, 2] and the Constrained Finite Strip Method (cFSM) [3]. The only problem is that they present limitations when dealing with arbitrary cross-sections and boundary/loading conditions. Even if recently, solutions were developed for many cases of loading and boundary conditions (e.g. [4, 5]), publicly available codes are not yet released (the available codes as GBTUL [6] and CUFSM [7] can handle nowadays only *bar* classical loading and boundary conditions).

As for perforated members, the specialised methods usually take into account the effect of the holes by introducing the concept of *reduced thickness* of the perforated strip ([8, 9]). Even if satisfactory results have been reported, this procedure could be criticized for using an unperforated model, disregarding the stress concentrations around the holes. It would be also impossible to apply this procedure for the case of uneven distribution or size of the holes.

Fig. 1 – Rack system.

On the other hand, the general solution methods, like Finite Element Method cannot explicitly provide the contribution of the pure deformation modes in a general buckling mode. The shell Finite Element Analysis (FEA) is the most commonly used instrument to study the behaviour of thin-walled members. Recently, an original method based on Generalised Beam Theory (GBT) was developed by the author [10] in order to decompose the elastic buckling modes provided by the shell FEA into pure buckling modes of Global, Distortional and Local nature. The main feature of this method lies in using only the GBT cross-sectional deformation modes instead of member mode shapes.

One goal of this paper is to present the latest developments which enable the modal identification method to analyse isotropic thin-walled members with arbitrary holes in terms of shape (rectangular and *circular*). The second goal is to study the effect of holes on the critical elastic resistance of perforated thin-walled members, which could lead in the near future to an optimisation procedure with respect the perforations distribution and shape for a given member.

2. GENERALISED BEAM THEORY – SHORT PRESENTATION

Figure 2 presents the terminology of the local coordinate system and the corresponding displacement field used for the study of thin-walled members with arbitrary cross-section.

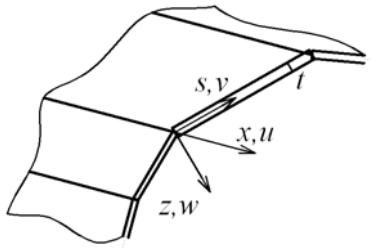

Fig. 2 – Thin-walled member: local axes/displacements.

In classical GBT, one assumes the classical Kirchhoff-Love hypotheses ($\varepsilon_{zz} = \gamma_{xz} = \gamma_{yz} = 0$) and also Vlasov's simplifying hypotheses (null membrane transverse extensions $\varepsilon_{ss}^{M,L} = \dot{v} = 0$ and membrane shear strains $\gamma_{xs}^{M,L} = \dot{u} + v' = 0$, where $(\,)' = \partial(\,)/\partial x$, $\dot{(\,)} = \partial(\,)/\partial s$. According to GBT, any displacement is considered as a linear combination of *n* orthogonal pure deformation modes, each one expressed as a product of two functions

$$\begin{aligned} u(s,x) &= \sum_{k=1}^{n} u_k(s)\phi_k'(x), \\ v(s,x) &= \sum_{k=1}^{n} v_k(s)\phi_k(x), \\ w(s,x) &= \sum_{k=1}^{n} w_k(s)\phi_k(x), \end{aligned} \tag{1}$$

where $u_k(s), v_k(s), w_k(s)$ are the components of the cross-sectional deformation modes and $\phi_k(x)$ are the amplitude functions describing their longitudinal

variation. The number of pure deformation modes *n* depends on the cross-section type (unbranched, branched, open, closed, etc.), the number of fold-lines and intermediate nodes. The warping displacements *u(s)* are considered to have linear variation along the entire cross-section, a consequence of the Vlasov's simplifying assumptions.

The 1st GBT step (the cross-sectional analysis) provides the cross-sectional deformation modes. Figure 3 presents the in-plane deformations of the first 22 pure deformation modes for a typical rack section. Notice that there are 4 Global deformation modes (axial, bending and torsion deformations), 6 Distortional deformation modes and the rest are all Local deformation modes.

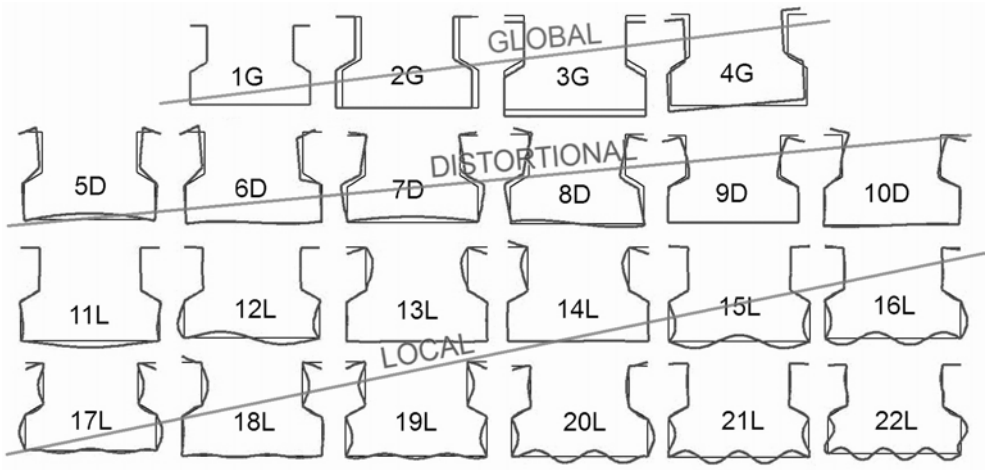

Fig. 3 – Rack section: the cross-sectional pure deformation modes.

Next, the member equilibrium equations are written based on the principle of virtual work applied in its variational form. The GBT system of differential equations in modal formulation has the expression [11]:

$$C_{ik}\phi_k^{IV} - D_{ik}\phi_k'' + B_{ik}\phi_k = \lambda X_{jik}\left(W_j^0\phi_k'\right)' \tag{2}$$

where *C*, *D*, *B* and *X* are the cross-section linear and geometrical stiffness matrices. The vector W^0 (having 4 components) contains the resultants of the applied pre-buckling stresses, namely (i) axial force ($W_1^0 = N$), (ii) bending moments ($W_2^0 = M_y$, $W_3^0 = M_z$), and (iii) bimoment ($W_4^0 = B$).

The GBT 2nd step (the member stability analysis) consists in solving the above differential equations system, yielding the critical load factors (λ) and the corresponding modal amplitude functions ($\phi_k(x)$). This step is not used by the method described in this paper.

3. BUCKLING MODE DECOMPOSITION FROM SHELL FEA

The described method extracts from a buckling shell FEA the amplitude functions $\phi_k(x)$ of the pure deformation modes. It is based on the special orthogonality properties of the cross-section deformation modes $u_k(s), v_k(s), w_k(s)$ and their derivatives. A special case of clear orthogonality can be seen if one analyses the transverse bending stiffness matrix *B* (a diagonal matrix):

$$B_{kk} = \int_s K\ddot{w}_k \ddot{w}_k ds = \int_s \frac{1}{K} m_k m_k ds \tag{3}$$

where $m_k(s) = -K\ddot{w}_k(s)$ are the cross-sectional transverse bending moments, $K = Et^3/(12(1-\mu^2))$ is the plate bending stiffness. The diagonal shape of matrix *B* proves the orthogonality properties of the 2nd derivatives of the cross-section displacements $w_k(s)$ or of the moments $m_k(s)$. In [10] the diagonal matrix *B* is used to extract from shell FEA the amplitude functions $\phi_k(x)$ of the Local and Distortional deformation modes. The procedure is now briefly presented for one simple example using a C-section member.

The modal identification method starts with a buckling shell FEA of a thin-walled member. Next, the cross-sectional displacement field is extracted on a mesh of points along the member's axis ($0 \le x_P \le L$, with *L* being the bar's length). Suppose that the general buckling FE deformation in one point *P* along the longitudinal axis of the member is given as a combination of three pure modes (3 – Global, 5 and 6 - Distortional) as presented in Fig. 4.

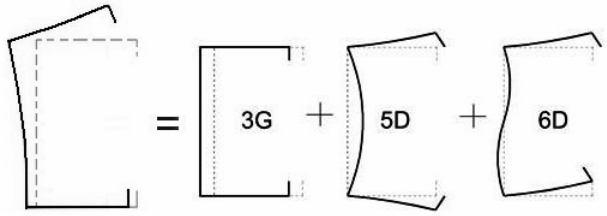

Fig. 4 – Combination of three pure modes.

From Eq. (1) the transversal displacements given by the shell FEA have the expression:

$$w_{FE}(s, x_P) = w_3(s)\phi_3(x_P) + w_5(s)\phi_5(x_P) + w_6(s)\phi_6(x_P) \tag{4}$$

and the transversal curvatures can be easily calculated

$$\ddot{w}_{FE}(s, x_P) = \ddot{w}_3(s)\phi_3(x_P) + \ddot{w}_5(s)\phi_5(x_P) + \ddot{w}_6(s)\phi_6(x_P) \tag{5}$$

Suppose we know the curvature functions $\ddot{w}_k(s)$ of all the cross-sectional deformation modes from the GBT 1st step and we can also extract the same functions from the shell FEA ($\ddot{w}_{FE}(s,x_P)$). In order to find the value of the amplitude function $\phi_6(x_P)$, we simply make the following integration

$$\begin{aligned}\int_s K\ddot{w}_6\ddot{w}_{FE}ds = \int_s K\ddot{w}_6(s)\ddot{w}_3(s)tds\cdot\phi_3(x_P)+\\ +\int_s K\ddot{w}_6(s)\ddot{w}_5(s)tds\cdot\phi_5(x_P)+\int_s K\ddot{w}_6(s)\ddot{w}_6(s)tds\cdot\phi_6(x_P)\end{aligned} \tag{6}$$

and because B is a diagonal matrix, we know that

$$\int_s K\ddot{w}_i\ddot{w}_k ds = 0 \text{ for any } i \neq k \tag{7}$$

so, the first two terms of Eq. (6) will be eliminated, thus giving

$$\int_s K\ddot{w}_6\ddot{w}_{FE}ds = \int_s K\ddot{w}_6(s)\ddot{w}_6(s)tds\cdot\phi_6(x_P) = B_{66}\phi_6(x_P) \tag{8}$$

Finally, the value of the amplitude function in point P is found

$$\phi_6(x_P) = \frac{\int_s K\ddot{w}_6\ddot{w}_{FE}ds}{B_{66}} \tag{9}$$

In [10] the computation of the integral from the above equation is explained in detail. The above described procedure can be used to identify all the pure buckling modes which involve cross-sectional distortions (D and L modes), using the general formula

$$\phi_i(x_P) = \frac{\int_s K\ddot{w}_i\ddot{w}_{FE}ds}{B_{ii}} \text{ for } i \geq 5 \tag{10}$$

This is not the case of the Global deformation modes (i = 1…4) involving axial extension, major/minor axis bending and torsion. For this reason, two different stiffness matrices introduced by Eq. (2) are currently used, the warping stiffness matrix C (a diagonal matrix) and the geometrical stiffness matrix X_1 (not diagonal) standing for the stiffness degradation due to pre-buckling axial compression. Their expressions are given below (for matrix C we have Membrane and Bending components):

$$\begin{aligned}C_{ik} = C_{ik}^M + C_{ik}^B = E\int_s tu_iu_k ds + \int_s Kw_iw_k ds\\ X_{1ik} = -\frac{1}{A}\int_s (v_iv_k + w_iw_k)tds\end{aligned} \tag{11}$$

where A is the cross-sectional area. Similarly with the procedure described above, matrix X_1 is used for the extraction of the amplitude functions $\phi_k(x)$ for all pure deformation modes, and matrix C is used for the derivatives of the amplitude functions $\phi_k'(x)$ which are needed for the description of the warping displacements (see Eq. (1a)). This process was recently described in detail in [12].

Having the amplitude functions and their derivatives, the entire displacement field (d_{GBT}) is recreated and compared with the initial one (d_{FE}), extracted from shell FEA. An error vector is constructed $d_{err} = d_{FE} - d_{GBT}$ and the approximation error of the proposed method is measured as the norm of the error vector relative to the norm of the FE displacement vector (an estimation criterion also used by Adany *et al*. [13]):

$$error = \frac{\sqrt{{d_{err}}^T d_{err}}}{\sqrt{{d_{FE}}^T d_{FE}}} \tag{12}$$

Finally, the method provides the modal identification and participation, the goal of the entire procedure, using the same formula proposed by Silvestre *et al*. [14], an easy and intuitive expression based only on the amplitude functions. The modal participation factor (P_i) is introduced as follows:

$$P_i = \frac{\int_L |\phi_i(x)| dx}{\sum_{k=1}^{n} \int_L |\phi_k(x)| dx} \tag{13}$$

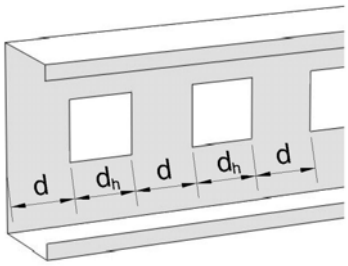

Fig. 5 – Thin-walled member: continuous and perforated regions.

One goal of this paper is to present the extension of the modal identification method for the special case of perforated thin-walled members with arbitrary holes. First, the member is divided in distinct regions along its length as shown in Fig. 5: continuous regions given by the intervals d, and regions with holes given by the intervals d_h.

These intervals don't have to be equal, there are no theoretical limitations concerning the shape, size and distribution of the holes. The buckling shell FEA is performed and the displacement field is extracted for each buckling mode

considered in the analysis. For any cross-section P ($0 \leq x_P \leq L$) inside the continuous regions, the method described in the previous section can be directly applied. For the perforated regions, the method can be applied if a minor modification is performed, taking into account the missing segments along the cross-section. The cross-sectional deformation modes remain the same, so the GBT 1st step is still applied for the continuous cross-section. The modification is introduced with respect the stiffness matrices. Basically, the components of these matrices are given by the virtual work produced by unit values of the amplitude functions, or their derivatives. So, for each missing segment, the virtual work is eliminated, meaning the integrals of Eq. (11) are calculated only on the "real" cross-sections of the perforated regions.

Concerning the shape and pattern of holes, the simplest case to apply the modal identification method described in this paper, is for members with rectangular holes regularly distributed along the member's length as presented in Fig. 6 (left side).

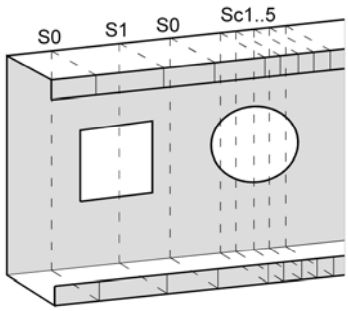

Fig. 6 – Thin-walled member with rectangular and circular holes.

In this case there are only two cross-sections that need to be analysed, one for the continuous (S_0) and one for the perforated regions (S_1), yielding two sets of stiffness matrices. However, the method has no theoretical limitations for non-regular patters and arbitrary shapes of holes. The complications are just of technical order, a circular hole will force the analysis of more than one cross-section along the perforation (Sc1..5). This technical detail is currently solved as it can be see in the illustrative example.

This is not the only technical complication; the circular holes (or rectangular holes with round corners) will produce an irregular FE mesh. The shell FEA displacement field is extracted in the FE nodes and in order to apply the mode decomposition method, the cross-sectional discretisations in shell FEA and GBT 1st step, have to be identical (an easy task for a regular FE mesh). For an irregular FE discretisation (Fig. 7), the GBT and FEA discretisations are different and the shell FEA displacement field has to be adapted by interpolation on the GBT mesh of points, keeping the approximation errors to a minimum, a task that is currently under work.

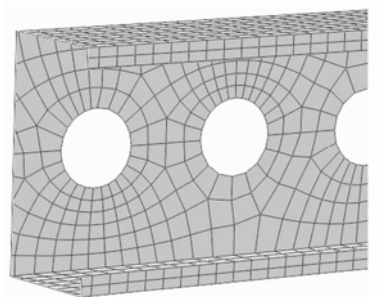

Fig. 7 – Irregular FE mesh for circular holes.

4. ILLUSTRATIVE EXAMPLE

The parametric study is completed on an axially compressed typical storage rack steel upright with and without holes. Assuming that this lipped channel is a cold-formed member, the thickness t = 2 mm is constant for all walls. The bar's length is L = 1500 mm, the material properties are: Young's modulus E = 210GPa and Poisson's ratio μ = 0.3 and cross-sectional dimensions are given in Fig. 8. The member is locally pinned at one end and simple-supported (meaning pinned locally and globally) and free to warp at the other end. The simple-supported end is axially compressed by an edge uniform load which gives a resultant force of 1kN. Seven perforation patterns were analysed as presented in Fig. 8. The first one (R0h) is without holes, the next 5 display different configurations of rectangular holes, and the last one displays circular holes. The name of the perforated members with rectangular holes is constructed as follows: 'R'(from "rack") + number of holes along the cross-section + 'rh' (from "rectangular hole") + hole transversal dimension. The 5th configuration presents 3 rectangular holes, 1 on web, 2 on flanges, and the 6th configuration presents 5 rectangular holes, 1 on web, 4 on flanges. All the rectangular holes have the longitudinal dimension of 50mm and the longitudinal center-to-center hole spacing of D = 90 mm. For circular holes, the radius is R = 30 mm and the longitudinal center-to-center hole spacing is the same D = 90 mm. The holes position and dimensions are chosen in such a way that the same material quantity is removed for each configuration. In this way, the influence of perforation pattern can be analysed from the point of view of critical load and also of the pure modes participation provided by the modal identification method presented in this paper. Local buckling is always preferable knowing that it has the best post-buckling strength reserve. From this point of view the Global buckling is the most unfavourable case, and the Distortional buckling is the intermediate case.

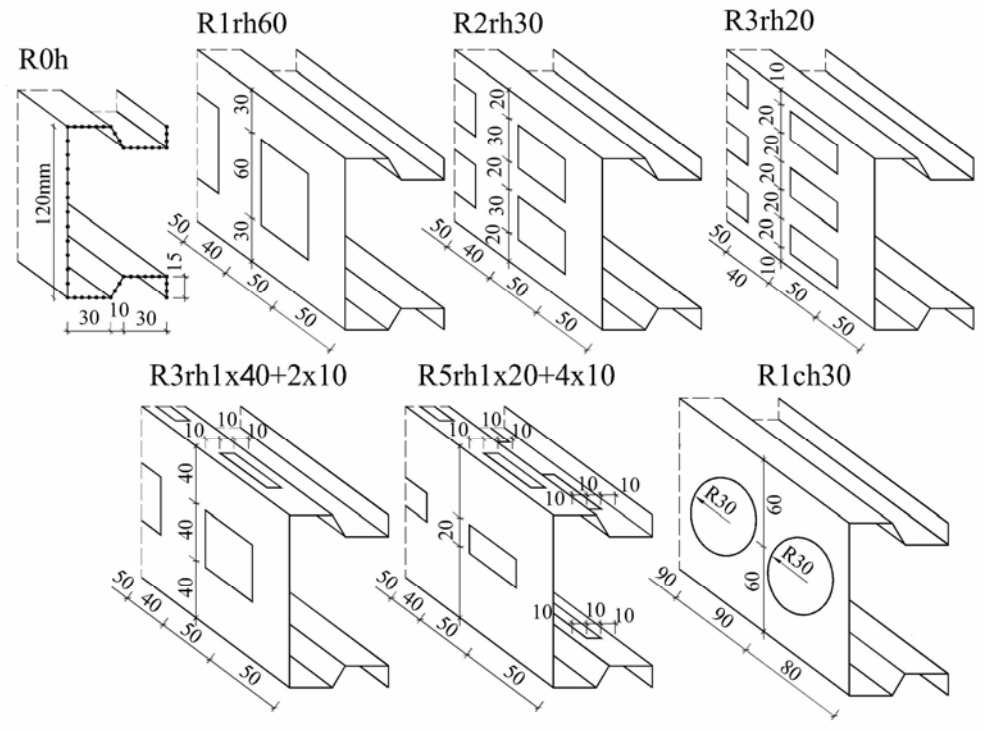

Fig. 8 – The analysed perforation patterns.

Buckling shell FEA of the thin-walled members were performed using ABAQUS [15] for the first 50 eigenvalues. Rectangular S4 shell finite elements were considered in a highly regular mesh, size L_{FE} = 10 mm in longitudinal direction, with the exception of the member with circular holes. For the last one, a special application was developed in MATLAB [16] which creates the Abaqus input file (inp extension) and in which the FE discretisation is introduced as regular as possible (see the last buckling shape of Fig. 13) otherwise it is quite difficult not to obtain complicated FE meshes as given in Fig. 7. For the continuous regions the cross-sectional discretisation is constant along the member length and identical with the one used by the GBT cross-sectional analysis (Fig. 8): 2, 5-2-5 and 11 intermediate nodes between the corners, respectively in the flange lips, flanges and web. For perforated regions, the rectangular holes require the analysis of an extra cross-section – the stiffness matrices are modified as explained in the previous section. The circular holes of radius R = 30 mm, required the analysis of R/L_{FE} = 3 extra cross-sections (due to symmetry with respect the hole's centre).

The GBT cross-sectional analysis performed on the continuous cross-section provides a number of n = 51 pure deformation modes: 4 Global, 6 Distortional and 41 Local (the first 22 modes were presented in Fig. 3). In order to implement the

described method of buckling identification and to calculate the modal participation, another MATLAB application was written. It uses the FE displacement field of 151 cross-sections given by the shell FE sides normal to the member longitudinal axis.

Method validation. The analysis provides the pure modes participation based on Eq. (13) for the first 50 general buckling modes provided by shell FEA and also the approximation error based on Eq. (12). Fig. 9–11 present these results for member configurations R0h (max. error = 1.32%), R1rh60 (max. error = 2.54%) and R1ch30 (max. error = 5.93%).

For all seven configurations, the maximum approximation error was the last one (5.93% for circular holes), buckling mode no. 38 caused by the local buckling of a very small region of the member. The higher value of the approximation error is due mainly to the simplifying assumptions introduced by the conventional GBT, especially the Vlasov's hypotheses and the linear variation of the warping displacements $u(x,s)$ according the s axis. Refining the longitudinal mesh and the GBT cross-sectional discretisation improves the accuracy of the presented method but not to drastic values (detailed explanations of this phenomenon are given in [17]). Nowadays GBT was extended in order to handle non-linear variation of the warping displacements along the cross-section wall midline, and also can take into account the cross-section deformations due to the wall transverse extensions. New pure modes are introduced, namely shear modes and transverse extension modes. The implementation of these two features will further improve the precision of the presented method, and is currently under work.

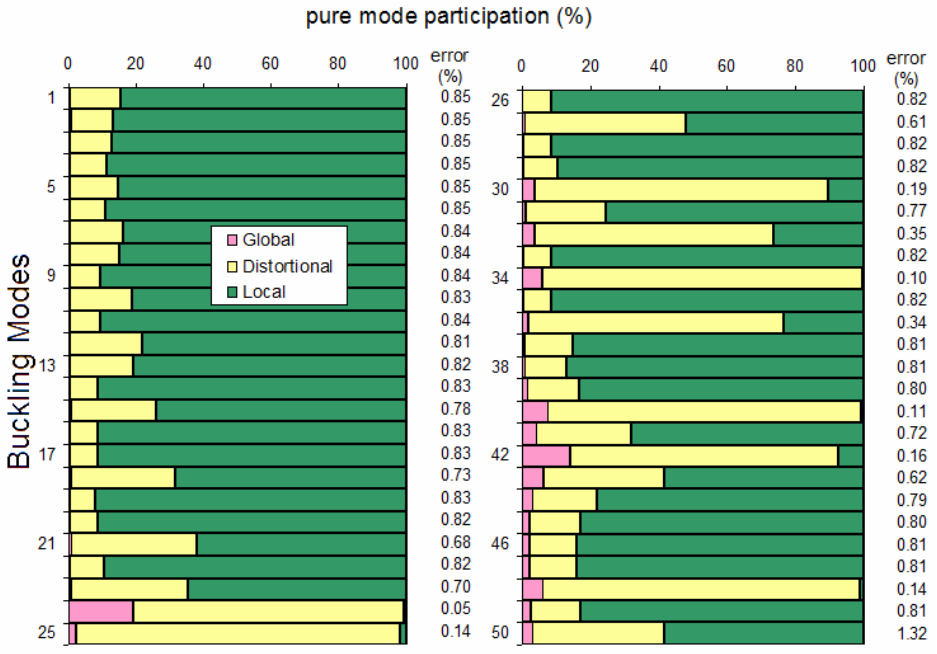

Fig. 9 – Member R0h: pure modes participation and approximation errors.

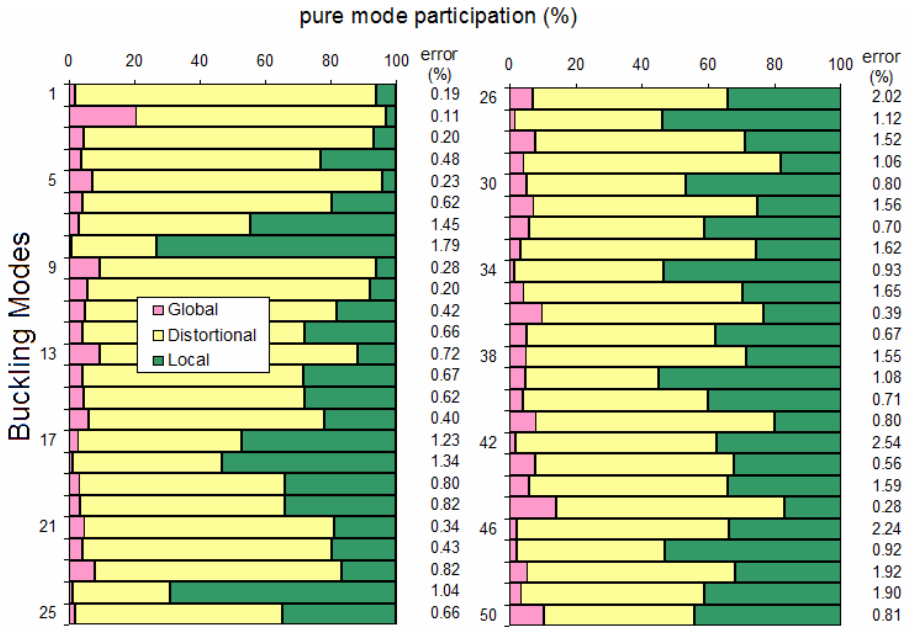

Fig. 10 – Member R1rh60: pure modes participation and approximation errors.

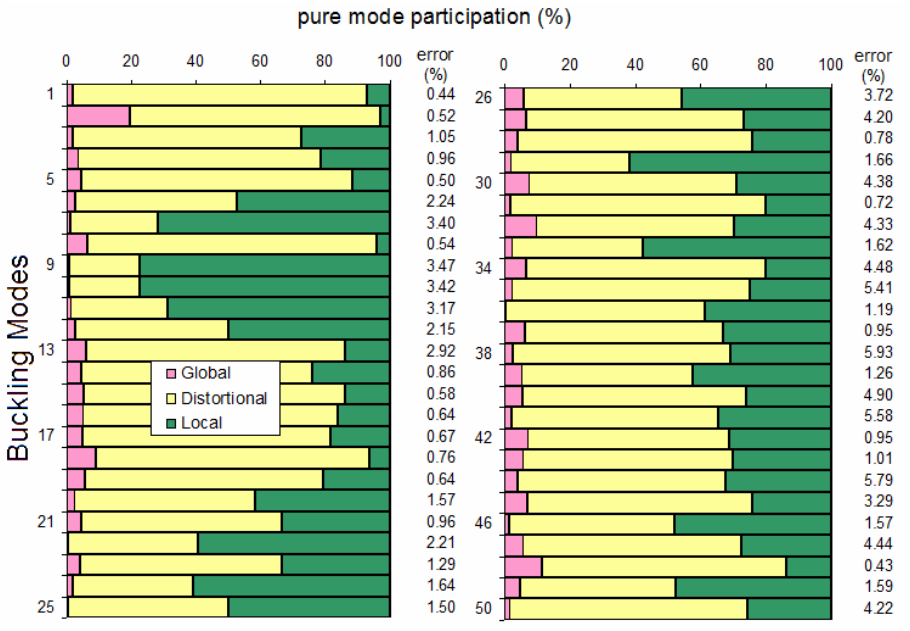

Fig. 11 – Member R1ch30: pure modes participation and approximation errors.

The effect of the perforation pattern. For all seven configurations, the 1st general buckling mode is analysed. Figure 12 presents the effect of the perforation pattern based on two factors: the pure modes participation and the critical load.

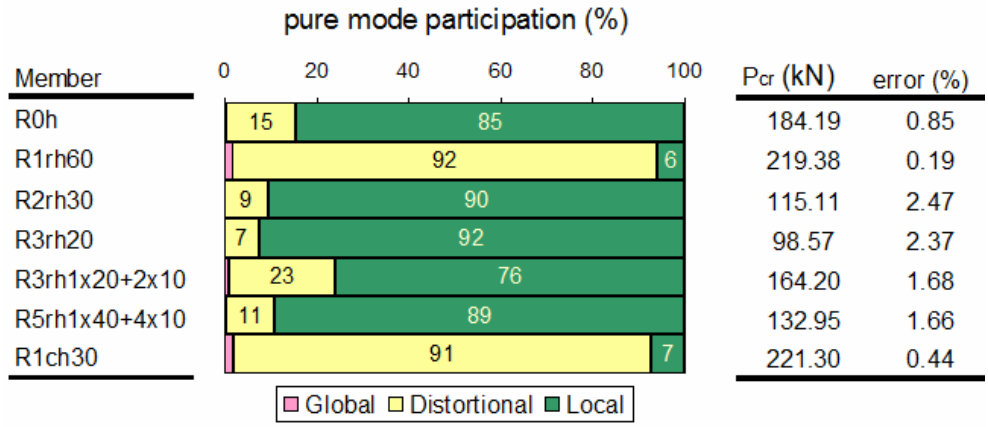

Fig. 12 – 1st general buckling mode: modal identification, critical load and approximation errors.

Figure 13 presents the deformed shape of the 1st shell FEA buckling mode for all seven configurations, together with the corresponding normalised amplitude functions $\phi(x)$ of the first most significant pure modes based on their participation provided by the presented method. The loaded and simply-supported end is at the left side.

It can be concluded from the numerical and visual results given in the last 5 figures that for this member, by placing only one large hole in the middle of the cross-section will highly favour the Distortional buckling and the critical load will actually increase in comparison with the unperforated member, a phenomenon already reported in literature (e.g. [18]). The Local deformations decrease, because the longitudinal normal stresses are directed through the top and bottom regions of the web, which are much stiffer due to their interaction with the flanges. In the same time the Distortional buckling decreases the post-buckling strength reserve. By placing 2 or 3 holes on the web will produce almost only Local buckling of the members, due to the unstiffened web regions between the holes, but the critical load is drastically decreasing. Placing a small-medium hole in the web leads to a Local-Distortional coupled instability.

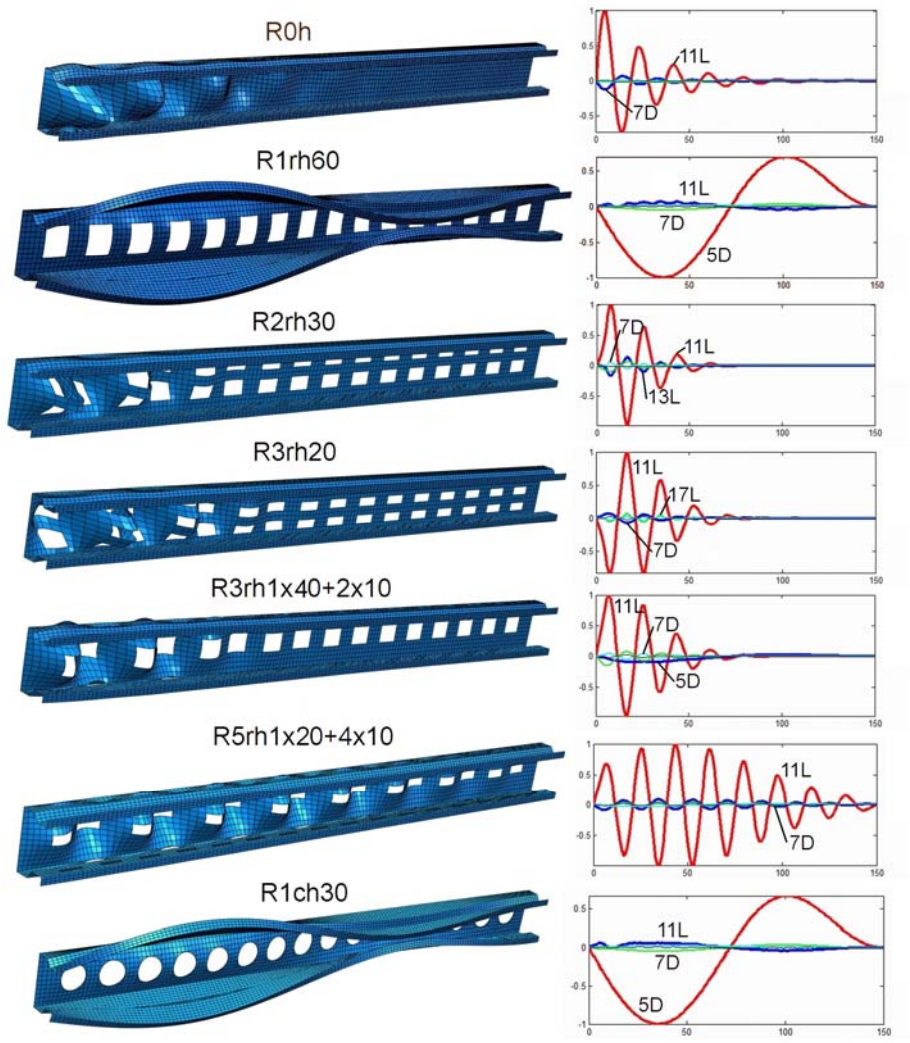

Fig. 13 – 1st FEM buckling mode and the amplitudes of the most relevant pure deformation modes.

One application of the presented method could be, in future, as follows: having the coupling quantified, the user can try other perforation patterns to find the optimal configuration which will provide the greatest participation of the Local buckling for an acceptable value of the critical load. Of course this procedure must be validated by geometric and material nonlinear collapse analyses (capable to provide the real response and the post-buckling behaviour of the member) also using the modal identification method described in this paper, a study that is currently under work.

4. CONCLUSIONS

This paper presents the latest developments of a GBT-based method (originally developed in [10]) capable of identifying in a general buckling mode provided by shell FEA, the modal participation of the pure deformation modes of Global, Distortional and Local type. This modal identification is a valuable quantitative tool for assessing coupled instabilities and the effect of perforation patterns. Its high speed must also be mentioned, and depends almost entirely of the time required by the shell FEA. For all these reasons, the proposed method is elegant, extremely fast and a promising candidate to be combined with a general purpose finite element code, providing in this way the buckling mode identification for arbitrary thin-walled members with and without holes.

Receveid on July 16, 2014

REFERENCES

1. SCHARDT, R., *Verallgemeinerte Technische Biegetheorie* (in German), Springer-Verlag, Berlin, 1989.
2. SCHARDT, R., *Generalized beam theory – an adequate method for coupled stability problems*, Journal of Thin-Walled Structures, **19**, pp. 161-180, 1994.
3. ÁDÁNY, S., SCHAFER, W. B., *A full modal decomposition of thin-walled, single branched open cross-section members via the constrained finite strip method*, Journal of Constructional Steel Research, **64,** pp. 12–29, 2008.
4. BASAGLIA, C., CAMOTIM, D., SILVESTRE, N., *Non-linear GBT formulation for open-section thin-walled members with arbitrary support conditions*. Journal of Computers and Structures, **89**, *21–22*, pp. 1906–1919, 2011.
5. LI, Z., SCHAFER, B.W., *Buckling analysis of cold-formed steel members with general boundary conditions using CUFSM: Conventional and constrained finite strip methods*, 20th International Specialty Conference on Cold-Formed Steel Structures – Recent Research and Developments in Cold-Formed Steel Design and Construction, 2010.
6. BEBIANO, R., PINA, P., SILVESTRE N. and CAMOTIM, D. , *GBTUL – Buckling and Vibration Analysis of Thin-Walled Members*, DECivil/IST, Technical University of Lisbon (http://www.civil.ist.utl.pt/gbt), 2008.
7. *** *Elastic Buckling Analysis of Thin-Walled Members by Finite Strip Analysis*, CUFSM (http://www.ce.jhu.edu/bschafer/cufsm/).
8. DAVIES, J. M., LEACH, P., TAYLOR, A., *The design of perforated cold-formed steel sections subject to axial load and bending*, Journal of Thin-Walled Structures, **29**, pp. 141–157, 1997.
9. MOEN, C., SCHAFER, W. B., *Direct strength method for design of cold-formed steel columns with holes,* Journal of Structural Engineering, **137**, *5*, pp. 559–570, 2011.
10. NEDELCU, M., *GBT-based buckling mode decomposition from finite element analysis of thin-walled members*, Journal of Thin-Walled Structures, **54**, pp. 156–163, 2012.
11. BEBIANO, R., SILVESTRE, N., CAMOTIM, D., *GBT formulation to analyze the buckling behaviour of thin-walled members subjected to non-uniform bending*, Journal of Structural Stability and Dynamics, **7**, *1*, pp. 23–54, 2007.

12. NEDELCU, M., CHIRA N., CUCU, H.L., POPA A.G., *Buckling mode decomposition of thin-walled members with holes*, 5th International Conference on Structural Engineering, Mechanics and Computation, Cape Town, South Africa, 2-4 September 2013.
13. ÁDÁNY, S., JOÓ, A., SCHAFER, W. B., *Buckling modes identification of thin-walled members using cFSM base functions*, Journal of Thin-Walled Structures, **48**, pp. 806–817, 2010.
14. SILVESTRE, N., CAMOTIM, D., *Second-order generalised beam theory for arbitrary orthotropic materials*, Journal of Thin-Walled Structures, **40**, pp. 791–820, 2002.
15. *** HIBBIT, KARLSSON & SORENSEN INC. ABAQUS Standard (Version 6.3), 2002.
16. *** MATLAB Version 7.1.0246 Documentation, The Mathwork Inc., 2005.
17. NEDELCU, M., CUCU H. L., *Buckling modes identification from fea of thin-walled members using only GBT cross-sectional deformation modes*, Journal of Thin-Walled Structures, Article in Press, 2013.
18. MOEN C., SCHAFER, W. B., *Elastic buckling of cold-formed steel columns and beams with holes*, Journal of Engineering Structures, **31**, *12*, pp. 2812–2824, 2009.